

## Neuronal algorithms that detect the temporal order of events

Gonzalo G. de Polavieja\*

*Neural Processing Laboratory, Instituto 'Nicolas Cabrera' & Department of Theoretical Physics,  
Universidad Autonoma de Madrid, Spain*

(Dated: January 23, 2006)

One of the basic operations in sensory processing is the computation of the temporal order of excitation of sensors. Motivated by the discrepancy between models and experiments at high signal contrast, we obtain families of algorithms by solutions of a general set of equations that define temporal order detection as an input-to-output relationship. Delays and nonlinear operations are the basis of all algorithms found, but different algorithmic structures exist when the operations are multiplications, OR gates, different types of AND-NOT logical gates or concatenated AND-NOT gates. Among others, we obtain the Hassenstein-Reichardt model, a network using a multiplicative operation that has been proposed to explain fly optomotor behavior. We also find extensions of the Barlow-Levick model (based on a AND-NOT gate with delayed inhibition and non-delayed excitation as inputs), originally proposed to explain the bipolar cell response of the rabbit retina to motion stimuli. In the extended models there are two more steps, another AND-NOT gate and a subtraction or two subtractions, that make the model responsive only to motion. In response to low-contrast inputs, the concatenated AND-NOT gates or the AND-NOT gate followed by a subtraction in these new models act as the multiplicative operation in the Hassenstein-Reichardt model. At high contrast the new models behave like the Hassenstein-Reichardt model except that they are independent of contrast as observed experimentally.

## INTRODUCTION

What are the possible neural networks that determine whether a group of sensors  $A$  has been excited before a group  $B$  or viceversa? A study of this problem has been pursued in the auditory system of the barn owl (Carr & Konishi, 1988) and more quantitatively in the visual system of insects and vertebrates. When  $A$  and  $B$  are photoreceptors or groups of them looking at two different points in space, temporal order translates into direction of visual motion. Important behaviors like prey detection (Land & Collett, 1974), gaze stabilization (Hausen & Egelhaaf, 1989; Egelhaaf et al., 2002) and distance estimation (Esch & Burns, 1996; Srinivasan, Zhang & Bidwell, 1997) can depend on the ability to compute the direction of motion.

The first proposal for a network of temporal order detection was given by Exner (Exner, 1894). Quantitative models emerged later in the study of the computation of the direction of motion in the insect and vertebrate retinae. The first mathematical model was proposed by Hassenstein and Reichardt to account for the optomotor behavior of the *Chlorophanus* beetle and was later extended to the fly (Hassenstein & Reichardt, 1956; Reichardt, 1961). The model, illustrated in Figure 1(A), has two arms. The left arm consists of the coincidence detection of a delayed signal from  $A$  and the signal from  $B$ . This arm detects  $A \rightarrow B$  motion and the its mirror-symmetric arm analogously for  $B \rightarrow A$  motion. The two relevant operations for the detection of temporal order are a delay and a multiplication. The underlying biological network responsible for these operations remains elusive due to the complexity of the network and the small size of the neurons implicated. However, the electrophysiological properties of neurons in lobula plate, a ganglion postsynaptic to the neurons computing the direction of motion, are consistent with the Hassenstein-Reichardt (HR) model at low light contrast (see, e.g., Borst & Egelhaaf, 1989; Haag, Denk & Borst, 2004). In vertebrates there is better experimental access to the network implicated in motion detection. The Barlow-Levick model (BL) (Barlow & Levick, 1965), shown in Figure 1(B), has been proposed to explain extracellular recordings from the ganglion cells of the rabbit retina. Its main operations are a delay and an AND-NOT logical gate with excitation and delayed inhibition as inputs. The AND-NOT gate has an output only when there is a signal coming from  $A$  and not from a channel that delays the signal from  $B$ . This scheme then has  $A \rightarrow B$  motion as its preferred direction and  $B \rightarrow A$  motion as its null direction.

The underlying physiology of this model is, as for the HR model, unknown, but it involves amacrine cells (Euler, Detwiler & Denk, 2002; Taylor & Vaney, 2003). Two other models have made an impact on our understanding of motion detection, the energy model (Adelson & Bergen, 1985) and the gradient detector (Limb & Murphy, 1975). The algorithm of the energy model is known to be mathematically equivalent to the HR model (Adelson & Bergen, 1985). The gradient model detects image velocity and not only temporal order. An interesting relationship between models using multiplication and velocity estimation has been shown using a version of estimation theory within a statistical mechanics framework (Potters & Bialek, 1994). Optimal velocity estimation implies a smooth transition between a gradient scheme at high signal to noise ratio (SNR) and a multiplication scheme at low signal-to-noise ratio (Potters & Bialek, 1994). Behavioral experiments show that bees can detect velocity (Kirchner & Srinivasan, 1989; Srinivasan, Lehrer, Kirchner & Zhang, 1991) but no evidence for a model like the gradient detector has been found (see, however, discussions of their possible relevance in biological motion detection in Hildreth & Koch, 1987 and Srinivasan, 1990).

Although previous studies have greatly advanced our understanding by establishing a methodology, identifying key features (e.g. delay and nonlinearities), and explaining many aspects of motion coding and perception, some fundamental problems are still unsolved. The HR model works well for low contrast but is inconsistent with the observed independence of response on image contrast at high contrast values (Fermi & Reichardt, 1963; Buchner, 1976; Götz, 1964; Hengstenberg & Götz; Egelhaaf & Borst, 1989). The BL model has the serious problem of not being a proper motion detector as it also responds to static stimuli. Its output to motion in its preferred direction is the same as the excitation of a single receptor while its output to motion in the null direction is the same as the excitation of neither of the receptors. In the limit of small signals, the BL scheme reduces to a 'dirty multiplication' (Thorson, 1966; Torre & Poggio, 1978). In fact, a model similar to the HR scheme in Figure 1(A) but with BL AND-NOT gates instead of the multiplications was shown to have an output with a term that depends on single receptor activation minus the HR terms so further spatio-temporal processing is needed to make a proper motion detector (Thorson, 1966). Furthermore, we have yet to discover how a real neural circuit detects motion and in the two best studied examples, insects and ganglion cells in vertebrate retina, the neural structures involved appear more intricate and complicated than the models (Taylor & Vaney,

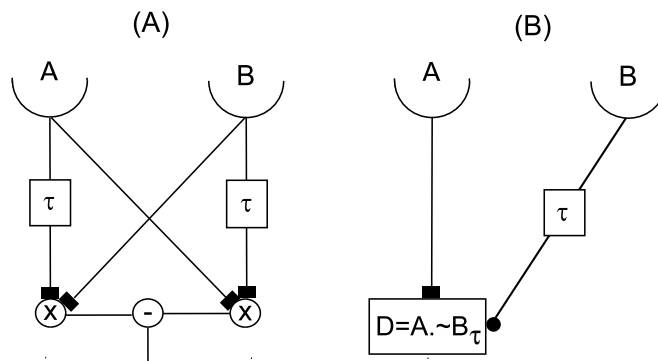


FIG. 1: Two models of temporal order detection have been obtained from experimental data. (a) Hassenstein-Reichardt model, obtained from the optomotor behavior of beetle and fly. Its main operations are a delay  $\tau$  and a multiplication. (b) Barlow-Levick model, proposed to explain the response of ganglion cells in the rabbit retina. Its main operations are a delay  $\tau$  and an AND-NOT logical gate with excitatory and delayed inhibitory inputs. The AND-NOT gate gives a non-zero output only when receiving a signal from  $A$  and not from a channel that delays the signal from  $B$  that we denote as  $B_{\tau}$ . Black squares (circles) indicate excitatory (inhibitory) inputs.

2003; Higgins, Douglass & Strausfeld, 2004).

There is a need to explore more ways to detect the temporal order of events. Here we propose a simple general procedure to obtain models of temporal order detection. It consists of translating the operation of a temporal order detector into a set of simultaneous equations whose solutions are the temporal order detection algorithms. We find families of models with a range of structures depending on the nonlinearities involved. These models are able to reconcile the apparent differences between the computational operations that are performed by the lateral excitation (HR) models and the lateral inhibition (BL) models. Algorithms that are extensions of the BL model are found that are proper motion detectors as they do not respond to the activation of single sensors. These models function like the HR model at low image contrast and are independent of contrast at high image contrast, converging to a value that depends on temporal frequency, as displayed by experimental data (de Ruyter van Steveninck, Bialek, Potters, Carlson, & Lewen, 1996).

The paper is organized as follows. First, we give the general procedure to obtain algorithms of motion detection. Second, we use this method to obtain different algorithmic structures depending on the nonlinearities used. Third, we show that some of these models are extended BL schemes and that they behave like the HR model at low contrast and are independent of contrast at high contrast. Finally we discuss the implications of the results in the study of neural circuitry involved in motion detection.

## SIMPLE METHOD TO OBTAIN ALGORITHMS THAT DETECT TEMPORAL ORDER

Our procedure involves translating the function of the network into an input-output relationship and obtaining the algorithms that obey it given a set of allowed operations. Consider a discrete space-time, say two points in space at time  $t - \tau$ ,  $A(t - \tau)$  and  $B(t - \tau)$ , and at time  $t$ ,  $A(t)$  and  $B(t)$ . There is motion from  $A$  to  $B$  when  $A$  is activated first and it is then followed by the activation of  $B$ . A simple representation of this is to say that  $A(t - \tau) = 1, B(t - \tau) = 0, A(t) = 0$  and  $B(t) = 1$ . There are 16 possible matrices of the discrete spatio-temporal input, represented in Figure 2. An algorithm for the detection of temporal order has to respond to these 16 inputs with the outputs given below the matrices in Figure 2. These output values mean that the algorithm cannot respond to static stimuli and that it has to distinguish  $A \rightarrow B$  from  $B \rightarrow A$  motion.

We are now ready to express the problem formally. For compactness, let  $\mathbf{A}(t - \tau)$  be the vector formed by the 16 matrix elements  $A(t - \tau)$  in the order given in Figure 2, and similarly for  $\mathbf{A}(t)$ ,  $\mathbf{B}(t - \tau)$  and  $\mathbf{B}(t)$ , and let  $\mathbf{R}$  be the vector of output values,

$$\begin{aligned}
 \mathbf{A}(t - \tau) &= (1, 0, 0, 1, 1, 0, 1, 0, 1, 1, 1, 0, 1, 0, 0, 0) \\
 \mathbf{A}(t) &= (0, 1, 0, 1, 1, 0, 0, 1, 1, 0, 1, 1, 0, 0, 1, 0) \\
 \mathbf{B}(t - \tau) &= (0, 1, 0, 1, 0, 1, 1, 0, 1, 1, 0, 1, 0, 1, 0, 0) \\
 \mathbf{B}(t) &= (1, 0, 0, 1, 0, 1, 0, 1, 0, 1, 1, 1, 0, 0, 0, 1) \\
 \mathbf{R} &= (1, -1, 0, 0, 0, 0, 0, 0, -1, 1, 1, -1, 0, 0, 0, 0). \tag{1}
 \end{aligned}$$

Having defined the input-output relationship, we need to restrict the possible operations among the elements of the input matrix. Consider two operations, the sum ‘+’ and the abstract operation ‘ $\odot$ ’, that in succeeding sections will be substituted by relevant nonlinear

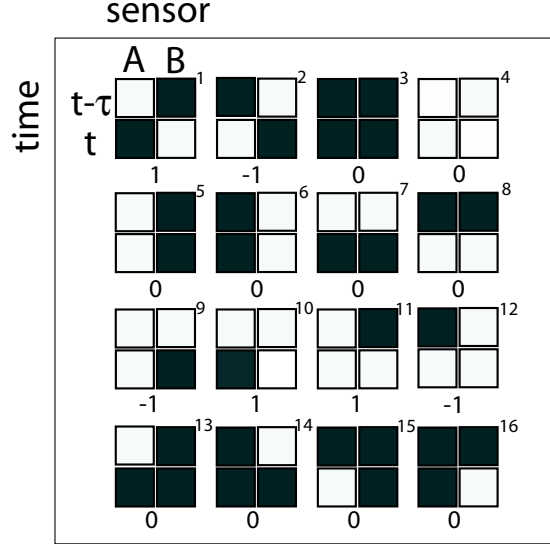


FIG. 2: The sixteen possible  $2 \times 2$  input matrices for binary detection elements and below them the outputs for an ideal temporal order detector. The first matrix, for example, has values  $A(t - \tau) = B(t) = 1$  represented in white and  $A(t) = B(t - \tau) = 0$  in black, corresponding to light exciting  $A$  first and then  $B$ . For this  $A \rightarrow B$  motion the output is 1. The second matrix corresponds to  $B \rightarrow A$  motion and has an output of  $-1$ .

operations like multiplications, OR gates, etc. We are interested in obtaining temporal order detectors using sums and the operation ' $\odot$ '. Formally, this consists of finding the parameters  $\{a, b, \dots, u\}$  that make the set operations with one or two matrix elements equal to the output vector  $\mathbf{R}$  when the inputs are those of the matrices in Figure 2, written in vector form in (1),

$$\begin{aligned}
\mathbf{R} = & a \mathbf{A}(t - \tau) + b\mathbf{A}(t) + c\mathbf{B}(t - \tau) + d\mathbf{B}(t) \\
& + e \mathbf{A}(t - \tau) \odot \mathbf{A}(t - \tau) + f\mathbf{A}(t) \odot \mathbf{A}(t) + g\mathbf{B}(t - \tau) \odot \mathbf{B}(t - \tau) + h\mathbf{B}(t) \odot \mathbf{B}(t) \\
& + i \mathbf{A}(t - \tau) \odot \mathbf{B}(t - \tau) + j\mathbf{A}(t - \tau) \odot \mathbf{B}(t) + k\mathbf{A}(t) \odot \mathbf{B}(t - \tau) + l\mathbf{A}(t) \odot \mathbf{B}(t) \\
& + m \mathbf{B}(t - \tau) \odot \mathbf{A}(t) + n\mathbf{B}(t) \odot \mathbf{A}(t - \tau) + o\mathbf{B}(t) \odot \mathbf{A}(t) + p\mathbf{B}(t) \odot \mathbf{A}(t) \\
& + q \mathbf{A}(t - \tau) \odot \mathbf{A}(t) + r\mathbf{A}(t) \odot \mathbf{A}(t - \tau) + s\mathbf{B}(t - \tau) \odot \mathbf{B}(t) + u\mathbf{B}(t) \odot \mathbf{B}(t - \tau), (2)
\end{aligned}$$

where the operations are entry-wise, i.e.,

$$\mathbf{A}(t - \tau) \odot \mathbf{A}(t) = (1, 0, \dots, 0) \odot (0, 1, \dots, 0) = (1 \odot 0, 0 \odot 1, \dots, 0 \odot 0). \quad (3)$$

Note that we have used the parameter  $u$  instead of the parameter  $t$  that would correspond

by the alphabetical order used to avoid confusion with the time  $t$ . Equation (2) will be used throughout this paper to obtain different models. When using commutative operations, that is when  $A \odot B = B \odot A$ , we do not need the terms with parameters from  $m$  to  $p$  and  $r$  and  $u$  as they would be redundant with other terms. Equation (2) contains all possible terms with one and two elements of the input matrices in Figure 2. Similar procedures can be used including the operation of three or four elements.

It is instructive to consider in some detail the procedure to find whether there exists a model using only the linear terms. This corresponds to the solutions of equation (2) without the operation ‘ $\odot$ ’ ( $e = f = \dots = u = 0$ ),

$$a\mathbf{A}(t - \tau) + b\mathbf{A}(t) + c\mathbf{B}(t - \tau) + d\mathbf{B}(t) = \mathbf{R}. \quad (4)$$

Substituting the vectors in (1) into (2), we obtain sixteen relationships between the four parameters  $a, b, c$  and  $d$  as

$$\begin{aligned} a + d = 0; b + c = -1; 0 = 0; a + b + c + d = 0; a + b = 0; c + d = 0; a + c = 0; b + d = 0 \quad (5) \\ a + b + c = -1; a + c + d = 1; a + b + d = 1; b + c + d = -1; a = 0; c = 0; b = 0; d = 0. \end{aligned}$$

It is however impossible to obey these sixteen relationships simultaneously. The last four relations require all the parameters to be zero while previous relations, for example the sixth and tenth, imply  $a = 1$ . Therefore no temporal order detection is possible with only the linear terms and we need to include a nonlinear operation ‘ $\odot$ ’, giving terms like  $+\mathbf{A}(t - \tau) \odot \mathbf{B}(t)$ . Systems of temporal order detection then need to operate input values at time  $t$  and at time  $t - \tau$ . For example, the term  $+\mathbf{A}(t - \tau) \odot \mathbf{B}(t)$ , can be computed by a system delaying the signal  $\mathbf{A}(t - \tau)$  by a time  $\tau$  to operate it with  $\mathbf{B}(t)$ . To write down the temporal detection algorithms from the point of view of the system we include the delay as a subscript, that is,

$$+\mathbf{A}(t - \tau) \odot \mathbf{B}(t) (\text{input operations}) \longrightarrow +\mathbf{A}_\tau \odot \mathbf{B} (\text{system operations}). \quad (6)$$

By considering a discrete space-time and binary inputs, the conditions for a motion detector are then given by sixteen relationships between parameters, as in equation (2). This procedure has the advantage, along with simplicity, of requiring only a minimal set of conditions. There are several extra conditions we do not impose, with the following advantages. First, we fix the output values only for discrete inputs. This allows us to obtain

models with different outputs when the input is a continuous signal. Second, we do not restrict the outputs when the inputs have negative values. This could be incorporated to equation (2) in a simple way, for example by requiring that the outputs remain the same when changing the sign of the input. However, vertebrate and insect retinae probably process differently motion detection for negative contrast, so we choose to leave open the behavior of the models for negative input. Finally, we do not model explicitly the ‘event detecting’ processing steps before temporal order detection. Some sensory systems first extract relevant features (i.e. bars or contours in the case of the visual system) and only later compute temporal order. However, basic features of the HR and the BL models compare well to experiments performed without the need of explicitly modeling the first sensory steps (i.e. photoreceptors and first interneurons) and we here follow the same strategy.

### HASSENSTEIN-REICHARDT MODEL AS THE SIMPLEST SOLUTION FOR A MULTIPLICATIVE NONLINEARITY

Substituting in equation (2) the abstract operation ‘ $\odot$ ’ for a multiplication ‘ $\times$ ’, our procedure involves finding the parameters that obey

$$\begin{aligned}
& a \mathbf{A}(t - \tau) + b\mathbf{A}(t) + c\mathbf{B}(t - \tau) + d\mathbf{B}(t) \\
& + e \mathbf{A}(t - \tau) \times \mathbf{A}(t - \tau) + f\mathbf{A}(t) \times \mathbf{A}(t) + g\mathbf{B}(t - \tau) \times \mathbf{B}(t - \tau) + h\mathbf{B}(t) \times \mathbf{B}(t) \\
& + i \mathbf{A}(t - \tau) \times \mathbf{B}(t - \tau) + j\mathbf{A}(t - \tau) \times \mathbf{B}(t) + k\mathbf{A}(t) \times \mathbf{B}(t - \tau) + l\mathbf{A}(t) \times \mathbf{B}(t) \\
& + q \mathbf{A}(t - \tau) \times \mathbf{A}(t) + s\mathbf{B}(t - \tau) \times \mathbf{B}(t) = \mathbf{R}.
\end{aligned} \tag{7}$$

We find a family of solutions obeying  $a = -e, b = -f, c = -g, d = -h, j = 1$ , and  $k = -1$  and zero for the remaining parameters. The simplest member of this family corresponds to  $a = b = c = d = 0$ , such that  $\mathbf{A}(t - \tau) \times \mathbf{B}(t) - \mathbf{B}(t - \tau) \times \mathbf{A}(t) = \mathbf{R}$ . Thus the simplest set of input operations that distinguish temporal order is of the form

$$A(t - \tau) \times B(t) - B(t - \tau) \times A(t). \tag{8}$$

As discussed in (6), these input operations correspond to the system operations

$$A_\tau \times B - B_\tau \times A, \tag{9}$$

that is the HR model, depicted in Figure 1(A).



In this paper we consider only the simplest solutions. For example, the algorithm  $A_\tau^2 - A_\tau + A_\tau \times B - B_\tau \times A$  is a valid solution for  $a = -e = -1$  but it only adds terms with no net output to the HR model. We do not consider models obtained with definitions of motion detection different to the one given in Figure 2. For example, we could consider a definition with null outputs for the inputs in the third row as they are neither clean motions nor static cases like the rest of the rows. This alternative definition would correspond to a substitution of  $\mathbf{R}$  in equation (2) for  $\mathbf{R}' = (1, -1, 0, 0, 0, 0, 0, 0, 0, 0, 0, 0, 0, 0, 0)$ . Models with this output contain terms operating three or four matrix elements. In the case of multiplications, the simplest model we find for this case is of the form

$$A_\tau \times B - B_\tau \times A + (A \times A_\tau \times B_\tau - A \times A_\tau \times B + A \times B \times B_\tau - A_\tau \times B \times B_\tau), \quad (10)$$

that adds four extra terms to the HR model found in (9) each with the multiplication of three matrix elements, a complexity that does not correspond to known biology.

#### OTHER MODELS WITH THE NONLINEARITY USING ONLY EXCITATION

To search for other algorithms for which the nonlinearity is also excitatory, we consider other operations. An AND logical gate with inputs  $x_1$  and  $x_2$ ,  $x_1 \wedge x_2$ , has an output of 1 when  $x_1 = x_2 = 1$  and zero otherwise. An AND gate can be realized biophysically with a spike threshold that is reached only when two excitatory inputs are active. The input-output of an AND gate is the same than that of the multiplication for binary inputs. Therefore our procedure finds the same models for AND gates and multiplications, the simplest being  $A_\tau \wedge B - B_\tau \wedge A$ .

An OR gate with inputs  $x_1$  and  $x_2$ ,  $x_1 \vee x_2$ , has an output of 1 when  $x_1 = 1$  or  $x_2 = 1$  or when both equal 1,  $x_1 = x_2 = 1$ , and zero otherwise. OR gates can be realized biophysically with a spike threshold lower than each of two excitatory inputs. Substituting the operation ‘ $\odot$ ’ in equation (2) by the operation ‘ $\vee$ ’, we find a solution corresponding to the system operations

$$A_\tau - B_\tau - A + B + A \vee B_\tau - A_\tau \vee B, \quad (11)$$

depicted in Figure 3(A). No experimental evidence for visual motion detection based on OR gates has been found so far.

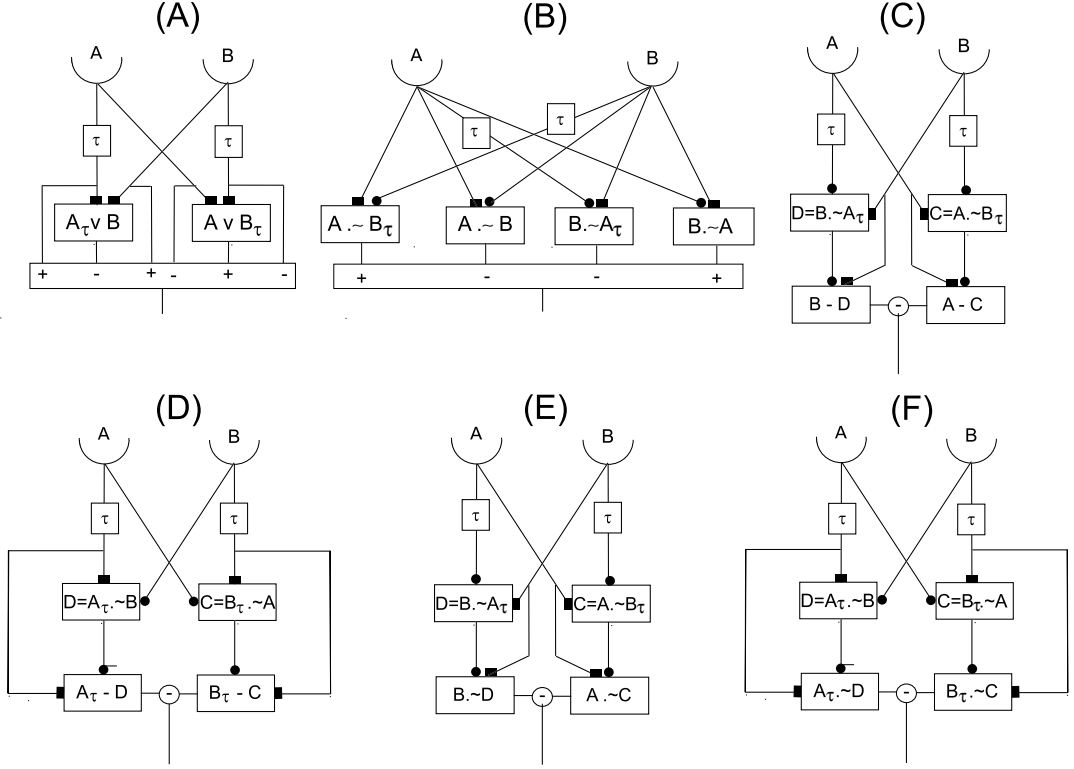


FIG. 3: Some network structures performing temporal order detection. (A,B) Two models of temporal order detection based on (A) OR gates and (B) AND-NOT gates. (C,D) Two models of temporal order detection with a first layer of AND-NOT gates and a second layer subtracting their output from the output coming from a single point in space. The Barlow-Levick model corresponds to the first layer of (C). (E,F) Two models using an concatenated AND-NOT gates. The Barlow-Levick model corresponds to the first layer of (E).

### MODELS WITH THE NONLINEARITY USING EXCITATION AND INHIBITION

The recordings implicated in the computation of visual motion detection are those found in the vertebrate retina (Barlow & Levick, 1965). In this case the relevant nonlinearity is the AND-NOT gate or a divisive operation (Amthor and Grzywacz, 1993; Grzywacz and Amthor, 1993). Anatomical evidence also points to the AND-NOT gate as a candidate operation in insect motion detection (Higgins, Douglass & Strausfeld, 2004). An AND-NOT gate with inputs  $x_1$  and  $x_2$  of the form  $x_1 \cdot \sim x_2$  has an output 1 only when  $x_1 = 1$  and  $x_2 = 0$  and zero otherwise. This is similar to a divisive operation  $x_1/x_2$ , that has a high value

(corresponding to the value 1 in the AND-NOT gate) only when  $x_1 = 1$  and  $x_2 = 0$  and low values otherwise (corresponding to the value 0 in the AND-NOT gate). The biophysics behind this operation could vary among systems. It could be based on the subtraction of excitatory an inhibitory inputs followed by a threshold, silent inhibition (Torre & Poggio, 1978) in non-spiking neurons (in spiking neurons silent inhibition only has a subtractive effect on the firing rate, see Holt and Koch, 1997), calcium enhanced calcium released (Barlow, 1996) or network effects (Holt and Koch, 1997).

### Models with AND-NOT gates and without linear terms

Substituting the operation ‘ $\odot$ ’ in equation (2) by the operation AND-NOT, we find a family of models without the linear terms and another family with them. Models without the linear terms ( $a = b = c = d = 0$ ) are obtained with parameters  $i = 1 - p, j = -1 + p, k = p, l = -p, m = p - 1, n = -p, o = 1 - p$  and zero for the remaining parameters. The simplest cases are obtained for  $p = 0$  and  $p = 1$ , corresponding, respectively, to the system operations

$$A_{\tau} \sim B_{\tau} - A_{\tau} \sim B - B_{\tau} \sim A_{\tau} + B_{\tau} \sim A \quad (12)$$

$$A \sim B_{\tau} - A \sim B - B \sim A_{\tau} + B \sim A. \quad (13)$$

Both models contain only AND-NOT gates, but only the second, depicted in Figure 3(B), contains BL interactions, represented by the terms  $A \sim B_{\tau}$  and  $B \sim A_{\tau}$ . However, this model also contains two other AND-NOT gates that do not have the BL structure.

### Models with AND-NOT gates and linear terms

We have obtained two simple models including linear terms. The first one has  $b = -1, d = 1, k = 1$  and  $n = -1$  and zero for the remaining parameters and obeys

$$B - (B \sim A_{\tau}) - \{A - (A \sim B_{\tau})\}, \quad (14)$$

depicted in Figure 3(C). The second model has  $a = 1, c = -1, j = -1$  and  $o = 1$  and zero for the remaining parameters, obeying

$$A_{\tau} - (A_{\tau} \sim B) - \{B_{\tau} - (B_{\tau} \sim A)\}. \quad (15)$$

shown in Figure 3(D). Combinations of any of the arms of these two models is also a solution, for example  $B - (B. \sim A_\tau). \sim A) - \{B_\tau - (B_\tau. \sim A)\}$ . The first of these two models, equation (14), is particularly interesting as it extends in a simple way the BL model to make it a proper motion detector. Its layer of AND-NOT gates has a pure BL structure and is sensitive to the direction of motion. The second layer has a structure with an inhibitory input from the first layer and excitation from a single receptor. This configuration reverses the preferred direction of the detector and eliminates responses to stimuli coming only from one receptor. The third step, a subtraction of the output from the two arms, eliminates the response to flicker affecting both receptors simultaneously. Note that the second and third steps can be interchanged without any consequence. Also note that the information from isolated sensors, e.g.  $B - A$  in (14), could be coming from operations involving other receptors, say  $C$  and  $D$ , that nevertheless do not respond in the  $A \leftrightarrow B$  direction. For example,  $B - A$  can be substituted for structures like  $B. \sim D - A. \sim C$  if  $C$  and  $D$  are not active in  $A \leftrightarrow B$  motion but could participate in the calculation of time order in the directions  $A \leftrightarrow C$  and  $B \leftrightarrow D$ , respectively.

### Models with concatenated AND-NOT gates

Given the relevance of the AND-NOT gates, we have also considered an extension of our procedure in equation (2) to include terms with the operation of three elements, in this case corresponding to concatenated AND-NOT gates. We find a model with concatenated AND-NOT gates of the form

$$B. \sim (B. \sim A_\tau) - A. \sim (A. \sim B_\tau), \quad (16)$$

represented in Figure 3(E). This model is similar to the one in (14) except that the output from the BL layer and the output from a single receptor meet at a second layer of AND-NOT gates. A second model is found to be of the form

$$A_\tau. \sim (A_\tau. \sim B) - B_\tau. \sim (B_\tau. \sim A), \quad (17)$$

that is depicted in Figure 3(F). This model is similar to the one in (15), except that the second layer also uses AND-NOT gates. The AND-NOT gates of this second model do not have the structure of the BL scheme. Combinations of any of the arms of these two models

is also a solution, for example  $B. \sim (B. \sim A_\tau) - B_\tau. \sim (B_\tau. \sim A)$ . The two models in equations (14) and (16), illustrated in Figures 3(E) and (F), are particularly interesting as their first layer of operations has a BL structure that is corrected in a second layer to make it a temporal order detector.

### RESPONSE OF THE EXTENDED BARLOW-LEVICK MODELS TO CONTINUOUS SIGNALS

The models obtained have the same input-output relationship for binary signals. For example, the HR model, equation (9), has the same input-output relationship than the extended BL models, equations (14) and (16). In particular, the multiplicative operation of the HR model has the same input-output relationship as the subtraction of the signal coming from a single receptor and an AND-NOT gate or as two concatenated AND-NOT gates,

$$A_\tau \times B = B - (B. \sim A_\tau) = B. \sim (B. \sim A_\tau). \quad (18)$$

However, the response of the models should differ for continuous signals and this helps us to identify which is used in nature. We are therefore interested in comparing their differences to known features of experimental data.

Motion experiments typically use a sinusoidal grating of mean intensity  $I_0$ , modulation  $\Delta I$ , velocity  $\omega$  and spatial period  $\lambda$ ,  $I(x, t) = I_0 + \Delta I \sin(2\pi(x - \omega t)/\lambda)$ . When the receptors  $A$  and  $B$  are separated by a distance  $\Delta x$  and the delay in the system is given by a first-order low-pass filter of time constant  $\tau$ , the signals arriving at the nonlinearity are of the form (Zanker, Srinivasan & Egelhaaf, 1999)

$$A(t) = I_0 + \Delta I \sin\left(\frac{2\pi\omega}{\lambda}t\right) \quad (19a)$$

$$A_\tau(t) = I_0 + F\Delta I \sin\left(\frac{2\pi\omega}{\lambda}t - \Phi\right) \quad (19b)$$

$$B(t) = I_0 + \Delta I \sin\left(\frac{2\pi\omega}{\lambda}(t - \Delta x/\omega)\right) \quad (19c)$$

$$B_\tau(t) = I_0 + F\Delta I \sin\left(\frac{2\pi\omega}{\lambda}(t - \Delta x/\omega) - \Phi\right) \quad (19d)$$

with  $F = (1 + (2\pi\omega\tau/\lambda)^2)^{1/2}$  and  $\Phi = -\arctan(2\pi\omega\tau/\lambda)$  the amplitude and phase response resulting from the filter, respectively. The time integral for the HR model then gives (Zanker,

Srinivasan & Egelhaaf, 1999)

$$\int_0^\infty dt(A_\tau(t) \times B(t) - B_\tau(t) \times A) = (\Delta I)^2 \sin(2\pi\Delta x/\lambda) \frac{\sin(\arctan(2\pi\omega\tau/\lambda))}{(1 + 4\pi^2\omega^2\tau^2/\lambda^2)^{1/2}}. \quad (20)$$

The output of the HR model to a sinusoidal grating has a simple form, the product of three terms. The first term depends only on contrast  $\Delta I$ , the second on the spatial period  $\lambda$  and the third on the temporal frequency  $\omega/\lambda$ . Similar results can be obtained using also a high-pass filter for the arm without delay (Buchner, 1976).

The first two columns in Figure 4 compare this output of the HR model to the output of the extended BL model in (14) of the form  $B - (B \sim A_\tau) - \{A - (A \sim B_\tau)\}$ . The AND-NOT gate with inputs  $x_1$  and  $x_2$  of the form  $x_1 \sim x_2$  can be written mathematically in terms of the Heaviside function  $\Theta(x_1 - x_2 - 1/2)$ , that is 0 when  $x_1 - x_2 - 1/2 < 0$  and 1 for  $x_1 - x_2 - 1/2 > 0$ . Biological implementations of the models must use smooth operations, and for this reason we use a smooth version of the Heaviside function of the form  $\Theta_s(x_1 - x_2) = (1 + \tanh(5((x_1 - x_2) - 1/2)))/2$ . Other parameters for this function or other smooth functions do not change qualitatively the results, for example the extrema of the output are the same. We expect different species to differ in the values of the parameters of this function. We have numerically calculated the time integral of the extended BL model using this smooth function and compared the results with the three terms resulting from the HR model in (20):

(a) *Term*  $\sin(2\pi\Delta x/\lambda)$ . At fixed temporal frequency  $\omega/\lambda$  and contrast  $\Delta I$ , the HR model has an output proportional to  $\sin(2\pi\Delta x/\lambda)$ . Figure 4(A) illustrates the output of the HR and the extended BL model in (14), respectively, against the inverse of the spatial period  $\lambda$  with a fixed temporal frequency  $\omega/\lambda = 20$  and contrast  $\Delta I = 0.4$  and the remaining parameters  $\tau = 5$ ,  $\Delta x = 2.5$  and  $I_0 = 0.5$ . Both models show a sinusoidal variation with extrema at  $1/\lambda = n/(4\Delta x)$  and  $n = \{1, 3, \dots\}$ .

(b) *Term*  $\sin(\arctan(2\pi\omega\tau/\lambda) (1 + 4\pi^2\omega^2\tau^2/\lambda^2)^{-1/2})$ . For fixed contrast  $\Delta I$  and spatial period  $\lambda$ , the HR model has an output proportional to  $\sin(\arctan(2\pi\omega\tau/\lambda) (1 + 4\pi^2\omega^2\tau^2/\lambda^2)^{-1/2})$ . Figure 4 (B) illustrates the output of the HR and extended BL models for  $\Delta I = 0.4$  and  $\lambda = 10$  and with the model parameters as before. There is again very good correspondence between the two models.

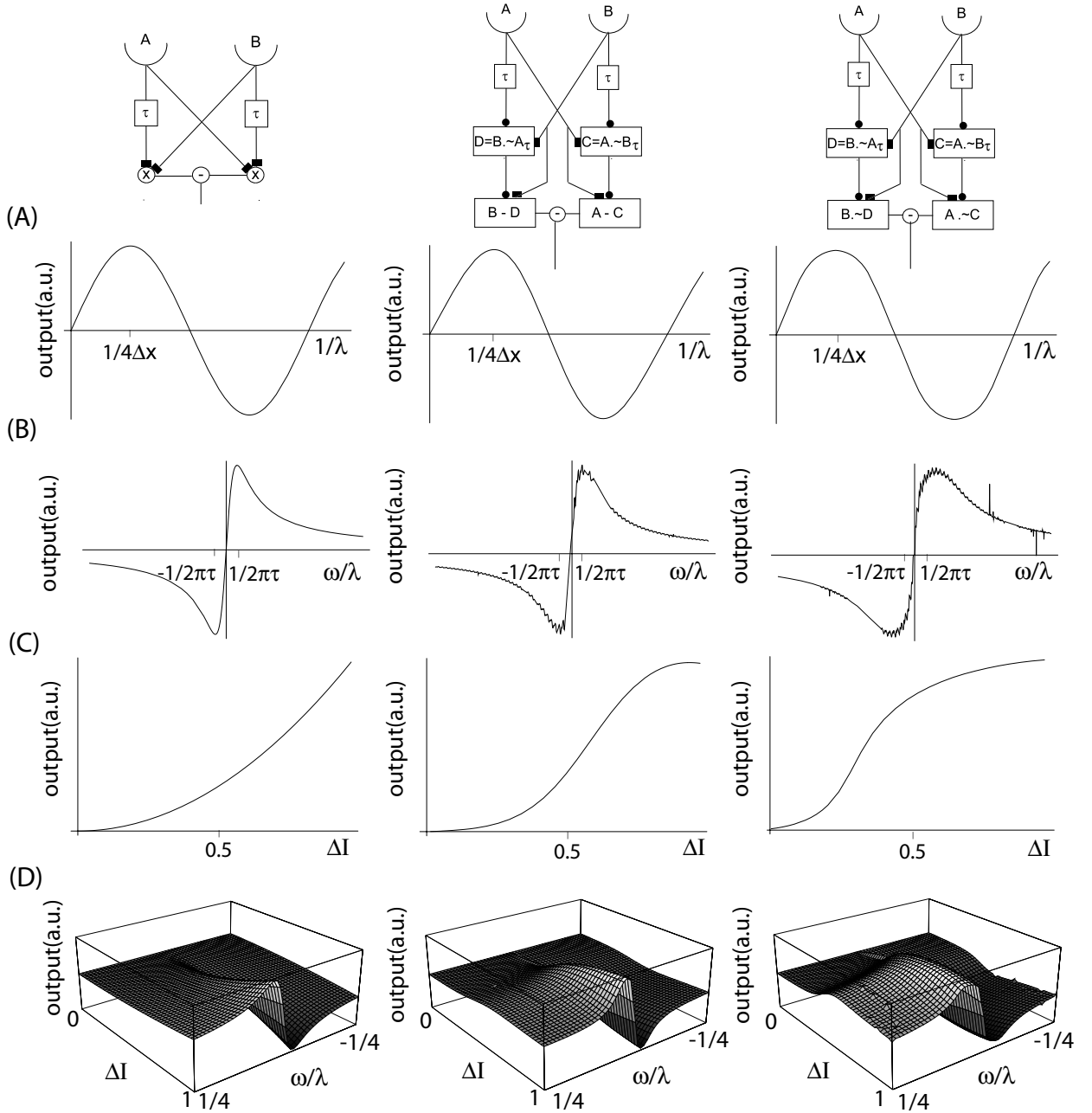


FIG. 4: Comparison of the output of the Hassenstein-Reichardt (left) and the extended Barlow-Levick models in equation (14) (middle) and (16) (right). The AND-NOT gates are smoothed using the function  $\Theta_s(x) = (1 + \tanh(5(x - 1/2)))/2$  for  $x > 0$  and zero for  $x < 0$ . Other parameters and smooth functions give similar results. (A) Output varying the spatial period  $\lambda$  for fixed temporal frequency  $\omega/\lambda = 1/20$  and fixed contrast  $\Delta I = 0.4$  and remaining parameters  $\tau = 5$ ,  $\Delta x = 2.5$  and  $I_0 = 0.5$ , chosen for illustrative purposes. (B) Output varying the grating velocity  $\omega$  at fixed contrast  $\Delta I = 0.4$  and spatial period  $\lambda = 10$ , and remaining parameters as in (A). (C) Output varying the contrast  $\Delta I$  at fixed spatial period  $\lambda = 20$  and velocity  $\omega = 0.5$ , and remaining parameters as in (A). (D) Same as (C) but showing that the output at high contrast is not saturated but converges to a value that depends on temporal frequency.

(c) *Term  $\Delta I^2$ .* Fixing the spatial period  $\lambda$  and velocity  $\omega$ , the HR model has an output proportional to  $\Delta I^2$ . Figure 4(C) gives the output of the HR and the extended BL model for  $\tau = 5, \Delta x = 2.5, I_0 = 0.5, \lambda = 20$  and  $\omega = 0.5$ . The extended BL model shows different behaviors at low and high contrast. While at low contrast it behaves similarly to the HR model, at high contrast it converges to an output value. Interestingly this convergence is not due to saturation, but instead its value depends on temporal frequency. Figure 4 (D) shows the output for the two models against contrast and velocity, clearly showing that the output of the extended BL model converges to a value that depends on temporal frequency.

The third column in Figure 4 gives the output for the extension of the BL model in (16). The results are similar to those in the second column, but with a slightly worse correspondence to the HR model. For example, it shows a maximum (minimum) at a value larger (lower) than  $\omega/\lambda = 1/(2\pi\tau)$  ( $\omega/\lambda = -1/(2\pi\tau)$ ).

Both of the extended BL models have an output very similar to that of the HR model, except for their contrast independency at high contrast, consistent with experimental data. It is important to note that the results do not depend qualitatively on the smoothing function. For example, using pure AND-NOT gates, the output depends on the inverse of the spatial period in a way similar to Figure 4(A) but with flatter output at the minima and maxima of the sine function. The output using pure AND-NOT gates also depends on contrast similarly to Figure 4(C) but with a more abrupt transition from the low contrast to the high contrast behavior. Also note that the results shown in Figure 4 need the full network structure of the extended BL models as single elements like an isolated AND-NOT gate have different outputs.

## DISCUSSION

We have given a general scheme to obtain models for the detection of the order of events as solutions of a set of simultaneous equations. Different families of network structures have been obtained depending on the nature of the nonlinearity they use. Models based on OR gates, different types of AND-NOT gates and concatenated gates have been given. This methodology can be used to obtain other algorithms by using other nonlinearities (logarithms, powers, etc) or by adding terms known to take place in real systems. We have



also shown that extended Barlow-Levick (BL) models function similarly to the Hassenstein-Reichardt (HR) model at low contrasts and are contrast independent at high contrast converging to a value that depends on temporal frequency, as displayed by experimental data (de Ruyter van Steveninck, Bialek, Potters, Carlson, & Lewen, 1996).

One of the lessons from this study is that there are several families of models that are able to perform the detection of the order of events. Their final outputs are similar and differences can always be minimized by adding extra elements. For example, even if the extended BL models obtained have been shown to have the contrast independency at high contrast, a modified Hassenstein-Reichardt scheme with contrast adaptation or a saturating nonlinearity can display similar behavior (Egelhaaf & Borst, 1989).

The relevance of having several models is therefore in making predictions for experiments designed to study the networks implicated in motion detection and not only their final output. For example, neurons participating in a motion detection network could be found firing for a shorter time in one direction of motion than in the opposite direction. While these neurons might not be thought to be critical neither in HR or extended BL schemes, they could be performing the processing of an OR gate, the most relevant processing step in a motion detection network like that of Figure 3(A).

A search for a network performing motion detection is in fact mostly a search for nonlinearities and delays. When physiological results show the existence of a nonlinearity, we can use models like those in Figure 3 to predict the existence of the other operations needed for the computation of motion detection. For example, in the case of finding an OR gate, the model in Figure 3(A) predicts that its output has to be subtracted from the sum of the delayed and non-delayed inputs. Other nonlinearities make different predictions. If an AND-NOT gate of the BL type (excitation and delayed inhibition as inputs) is found, the simplest models, Figures 3(C) and 3(E), predict that its output is compared to the undelayed line. On the other hand, when it is found an AND-NOT gate with inhibition and delayed excitation, as in Figures 3(D) and 3(F), it is predicted that its output is compared to the delayed line. In case AND-NOT gates are found without any delayed inputs, Figure 3(B) predicts that its output has to be mixed with outputs of different types of AND-NOT gates.

As an example of the predictive value of the models, in the following we discuss the predictions that the extended BL models make for the insect and vertebrate retinae given

our present knowledge. Most of the discussions on insect motion detection focus on the output of motion detectors as it is much easier to record from lobula plate neurons, that are postsynaptic to the motion detector networks believed to be in the medulla. However, a recent study has used anatomical and physiological data in medulla (Douglass & Strausfeld, 2001) to propose a model that maps to the HR scheme (Higgins, Douglass & Strausfeld, 2004). The HDS model has three steps. First, neuron T5 receives excitatory input from the trans-medullary neuron Tm1 (say, our B) and inhibitory input from Tm9 (our A), the latter acting as a low-pass filter. The HDS model assumes this interaction to be implementing a ‘dirty multiplication’ by shunting inhibition (Thorson, 1966; Torre & Poggio, 1978). Although less anchored in empirical evidence, the HDS model assumes two more steps. In the second step, the inhibitory input from an interneuron that receives the same input from two T5 cells (from the left and right arms of the model) returns a weighted inhibition to them. The final step is the spatial averaging, necessary to avoid the response to a single receptor. The extended BL models share with the HDS model the first step, in our case without the need to invoke the ‘dirty multiplication’ approximation that is only valid for low contrast. Neuron T5 would be then performing an AND-NOT gate with inputs from Tm1 and Tm9. The prediction of the model is that the output of this gate has to be further compared (by subtraction or a second AND-NOT gate) with information from T1. This second step could in principle take place in the dendritic tree of T5 in a shunting-inhibition model or in a different interneuron. For small inputs, the AND-NOT gate  $B. \sim A_\tau$  performed by shunting inhibition reduces to  $B(1 - A_\tau/I_{max})$  (Thorson, 1966; Torre & Poggio, 1978). The extended BL model can then be approximated at low contrasts by the Hassentein-Reichardt model,

$$B - (B. \sim A_\tau) - \{A - (A. \sim B_\tau)\} \approx (A_\tau B - AB_\tau)/I_{max}. \quad (21)$$

Other possibilities are open for motion detection in insects, like networks using AND-NOT gates with delayed excitatory and non-delayed inhibitory inputs like the one in Figure 3(D). This model predicts that the output of the AND-NOT gates has to be subtracted from the single-receptor delayed signal, and it also reduces to the HR model in the small signal limit of the shunting inhibition,

$$A_\tau - (A_\tau. \sim B) - \{B_\tau - (B_\tau. \sim A)\} \approx (A_\tau B - AB_\tau)/I_{max}. \quad (22)$$

Note that the HDS and our extended BL models work with positive numbers. In our case the models are solutions obtained for a binary input values ‘0’ and ‘1’, as shown in Figure

2. This means that inputs below zero are treated as the symbol ‘0’ and inputs above ‘0’ are treated as the symbol ‘1’. This procedure treats negative values as if they were a value of ‘0’. However, for a multiplication negative numbers matter, as  $\text{negative} \times \text{negative} = \text{positive}$ ,  $\text{negative} \times \text{positive} = \text{negative}$ . A simple way to achieve this behavior is to use four subsystems: ON-ON (A and B responding to light increases), OFF-OFF, ON-OFF and OFF-ON. This separation into channels is common to the HDS model, our extended BL model and has even been proposed as a silicon implementation of the HR model (see, e.g., Liu, 2000).

The vertebrate visual system also shows differences at low and high contrast. Humans perceive low-contrast gratings to be slower than high-contrast ones at the same velocity (e.g. Blakemore & Snowden, 1999). To understand the network implicated in motion detection we need to look for the neurons presynaptic to a motor system that respond differently depending on the external motion direction. The nucleus of the optic tract in the pretectum and the accessory optic system distinguish the direction of motion and connect to the motor system that controls eye movements. The role of these systems is probably to respond to wide-field stimulation by summing the responses of many motion detectors, as does the insect lobula plate (Krapp & Henstenberg, 1994). Neurons in the nucleus of the optic tract have an output that depends quadratically with contrast but at high contrast the response tends to a plateau (Ibbotson, Clifford & Mark, 1999), consistent with our extended BL models. Also note that the nucleus of the optic tract receives inputs from the ganglion cells, that can act as the AND-NOT gate of the pure BL model. The prediction of the extended BL models is then that the output of the AND-NOT gates in ganglion cells is subtracted from information non-motion information from one point in space. The outputs of these subtractions from the two arms in the models are further subtracted, in this case possibly in the nucleus of the optic tract.

## ACKNOWLEDGMENTS

I am very grateful to Horace Barlow, Brian Burton and Simon Laughlin for a critical and detailed reading of the manuscript and for many useful suggestions. Discussions with Sara Arganda, Raul Guantes, Mikko Juusola and Ignacio Ramis are also acknowledged. I thank the support of the program ‘Understanding the brain’ at KITP, Santa Barbara, and grants from the Wellcome Trust, MEC, fBBVA and CAM-UAM.

## BIBLIOGRAPHY

Adelson, E.H. & Bergen, J.R. (1985) Spatiotemporal energy models for the perception of motion, *J. Opt. Soc. Am. A* **2**, 284-299

Amthor, F.R. & Grywacz, N.M. (1993) Inhibition in On-Off directionally selective ganglion cells in the rabbit retina. *J. Neurophysiol.* **69**, 2174-2187.

Barlow, H.B. & Levick, W.R. (1965) The mechanism of directionally selective units in rabbit retina. *J. Physiol. (Lond)* **178**, 477-504.

Barlow, H.B. (1996) Intraneuronal information processing, directional selectivity and memory for spation-temporal sequences, *Network* **7**, 251-259.

Blakemore, M., & Snowden, R. J. (1999). The effect of contrast on perceived speed: a general phenomenon? *Perception*, **28**, 33-48.

Borst, A. & Egelhaaf, M. (1989) Principles of visual motion detection. *Trends Nuerosci.* **12**, 297-306.

Buchner, E. (1976) Elementary movement detectors in an insect visual system, *Biol. Cybern.* **24**, 85-101.

Buchner, E. (1984) Behavioral analysis of spatial vision in insects. In: *Photoreception and vision in invertebrates* (Ali, M.A., ed). Plenum, New York, 561-621.

Carr, C.E. & Konishi, M. (1988) Axonal delay lines for time measurement in the owls brainstem, *Proc. Nat. Ac. Sci.* **85**, 8311-8315.

de Ruyter van Steveninck, R.R., Bialek, W., Potters, M. Carlson, R.H. & Lewen, G.D. (1996) Adaptive movement computation by the blowfly visual system. In: *Natural and artificial parallel computation*, Proc. of the 5th NEC Research Symposium (D. Waltz, ed.)

SIAM Press, Philadelphia, PA, pp. 21-41.

Douglas & Strausfeld (2001) Pathways in dipteran insects for early motion processing, In: Zanker, J.M. & Zeil, J. (Eds.), *Motion Vision: Computational, Neural and Ecological constraints*, Springer, Berlin, 66-81.

Egelhaaf, M. & Borst, A. (1989) Transient and steady-state response properties of movement detectors, *J. of the Opt. Soc. of America* **6**, 116-127.

Egelhaaf, M., Kern, R., Krapp, H.G., Ketzberg, J., Kurtz, R. & Warzecha, A.K. (2002) Neural encoding of behaviorally relevant visual-motion information in the fly, *TINS* **25**, 96-102.

Esch, H. & Burns, J. (1996) Distance estimation by foraging honeybees, *J. Exp. Biol.* **199**, 155-162.

Euler, T., Detwiller, P.B. & Denk, W. (2002) Directionally selective calcium signals in dendrites of starburst amacrine cells, *Nature* **418**, 845-852.

Exner, S. (1894) Entwurf zu Einer Physiologischen Erklärung der Psychischen Erscheinungen. I. Teil. Deuticke, Leipzig, 37-140.

Fermi, G. and W.E. Reichardt (1963) Optomotorische Reaktionen der Fliege *Musca domestica*. *Kybernetik* **2**, 15-28.

Götz, K.G. (1964) Optomotorische Untersuchungen des visuellen Systems einiger Augenmutanten der Fruchtfliege *Drosophila*. *Kybernetik* **2**, 77-92.

Grywacz, N.M. & Amthor, F.R. (1993). Facilitation in On-Off directionally selective ganglion cells in the rabbit retina. *J. Neurophysiol.* **69**, 2188-2199.

Haag, J., Denk, W. & Borst (2004) Fly motion vision is based on Reichardt detectors regardless of the signal-to-noise ratio, *Proc. Nat. Acad. Sci.* **101**, 16333-16338.

Hassenstein, B. & Reichardt, W. (1956) Systemtheoretische analyse der Zeit-, Reihenfolgen- und Vorzeichenauswertung bei der Bewegungsperezeption des Russelkafers *Chlorophanus*, *Zeitschrift fur Naturforschung* **116**, 513-524

Hausen, K. & Egelhaaf, M. (1989) Neural mechanisms of visual course control in insects. In: *Facets of vision* (Stavenga, D., Hardie, R., eds), New York:Springer, pp. 391-424.

Hengstenberg, R. and K.G. Götz (1967) Der Einflu des Schirmpigmentgehalts auf die Helligkeits- und Kontrastwahrnehmung bei *Drosophila* Augenmutanten. *Kybernetik* **3**, 276-285.

Higgins CM, Douglass JK, Strausfeld NJ. (2004) The computational basis of an identified neuronal circuit for elementary motion detection in dipterous insects. *Vis. Neurosci.* **21**, 567-586.

Hildreth, E.C. & Koch, C. (1987) The analysis of motion: From computational theory to neuronal mechanisms. *Ann. Rev. Neurosci.* **10**, 477-533.

Holt, G.R. & Koch, C. (1997) Shunting inhibition does not have a divisive effect on firing rates. *Neural Comp.* **9**, 1001-1013.

Ibbotson, M.R., Clifford C.W.G. & Mark, R.F. (1999) A quadratic nonlinearity underlies direction selectivity in the nucleus of the optic tract, *Visual Neurosci.* **16**, 991-1000.

Krapp HG and Hengstenberg R (1996) Estimation of self-motion by optic flow processing in single visual interneurons. *Nature* **384**, 463-466.

Kirchner, W.H. & Srinivasan, M.V. (1989) *Naturwissenschaften* **69**, 281-282.

Koch, C. (1999) *Biophysics of Computation: Information processing in single neurons*. OUP.

Land, M.F. & Collett, T.S. (1974) Chasing behaviour of houseflies (*Fannia canicularis*). *J. Comp. Physiol.* **89**, 331-357.

Levick, W.R. & Oyster, C.W., Takahashi, E. (1969) Rabbit lateral geniculate nucleus: sharpener of directional information. *Science* **165**, 712-714.

Limb, J.O. & Murphy, J.A. (1975) Estimating the velocity of moving images in television signals. *Comp. Graph Im. Process.* **4**, 311-327

Liv, S-C. (2000) A neuromorphic aVSLI model of global motion processing in the fly. *IEEE Transactions on circuits and systems II: analog and digital signal processing* **47**, 1458-1467.

Potters, M. & Bialek, W. (1994) Statistical mechanics and visual signal processing. *J. Phys. I France* **4**, 1755-1775 (1994)

Reichardt, W. (1961) Autocorrelation, a principle for the evaluation of sensory information by the central nervous system. In: *Sensory Communication*, (Rosenblith, W.A., ed.), New York: Wiley, 303-317

Srinivasan, M.V. (1990) Generalized gradient schemes for the measurement of two-dimensional image motion. *Biol. Cybern.* **63**, 421-431.

Srinivasan, M.V., Lehrer, M., Kirchner, W.H. & Zhang, S.W. (1991), *Visual Neurosci.* **6**, 519-535.

Srinivasan, M.V., Zhang, S.W. & Bidwell, N. (1997) Visually mediated odometry in honeybees. *J. Exp. Biol.* **200**, 2513-2522.

Taylor, W.R. & Vaney, D.I. (2003) New directions in retinal research, *Trends in Neurosci.* **26**, 379-385.

Thorson, J. (1966) Small-signal analysis of a visual reflex in the locust II. Frequency dependence, *Kybernetik* **3**, 56-66.

Torre, V. & Poggio, T. (1978). A synaptic mechanism possibly underlying directional selectivity to motion. *Proc. Roy. Soc. London* **202**, 409-416.

Zanker, J.M., Srinivasan, M.V. & Egelhaaf, M. (1999) Speed tuning in elementary motion detectors of the correlation type. *Biol. Cybern.* **80**, 109-116.

---

\* [gonzalo.polavieja@uam.es](mailto:gonzalo.polavieja@uam.es); [http://www.ft.uam.es/neurociencia/gonzalo/Leech\\_page.htm](http://www.ft.uam.es/neurociencia/gonzalo/Leech_page.htm)